



Deposited via The University of Sheffield.

White Rose Research Online URL for this paper:

<https://eprints.whiterose.ac.uk/id/eprint/188881/>

Version: Published Version

Article:

Kumar, P., Legge, A., Gregory, D.A. et al. (2022) 3D printable self-propelling sensors for the assessment of water quality via surface tension. *JCIS Open*, 5. 100044. ISSN: 2666-934X

<https://doi.org/10.1016/j.jciso.2022.100044>

Reuse

This article is distributed under the terms of the Creative Commons Attribution (CC BY) licence. This licence allows you to distribute, remix, tweak, and build upon the work, even commercially, as long as you credit the authors for the original work. More information and the full terms of the licence here:

<https://creativecommons.org/licenses/>

Takedown

If you consider content in White Rose Research Online to be in breach of UK law, please notify us by emailing eprints@whiterose.ac.uk including the URL of the record and the reason for the withdrawal request.



3D printable self-propelling sensors for the assessment of water quality via surface tension



Piyush Kumar^a, Abigail Legge^b, David A. Gregory^c, Andy Nichols^b, Henriette Jensen^a, Stephen J. Ebbens^{a,**}, Xiubo Zhao^{a,d,*}

^a Department of Chemical and Biological Engineering, University of Sheffield, Sheffield, S1 3JD, UK

^b Department of Civil & Structural Engineering, University of Sheffield, Sheffield, S1 3JD, UK

^c Department of Material Sciences and Engineering, University of Sheffield, Sheffield, S1 3JD, UK

^d School of Pharmacy, Changzhou University, Changzhou, 213164, China

ARTICLE INFO

Keywords:

Inkjet printing
Self-propelling sensors
Water pollution
Contaminants
Surface tension
Marangoni effect

ABSTRACT

Hypothesis: Water contamination is a serious global challenge and an on-site and out-of-lab method of assessment of contamination level is highly needed. In this study, we report the potential of using printable and biodegradable propelling sensors as indicators of water contamination in sewage wastewater.

Experiments: We used reactive 3D inkjet printing technology to fabricate self-propelling sensors which can quickly indicate the lowering of surface tension value caused by sewage contamination, and other surface tension lowering pollutants. The Z-shaped sensors were fabricated, with the dimensions of 2.0 mm at the longest side and 0.1 mm in thickness, from regenerated silk fibroin which is an environmentally friendly and biodegradable material. Inkjet printing has the advantage of high resolution and precise deposition of materials allowing the fabrication of small millimetre-sized sensors doped with a surface tension modifying polymer which acts as the 'fuel' to drive the sensors on the water surface via surface tension gradient.

Findings: Our results showed that the sensor's propulsion velocity decay rate is an excellent metric to indicate the presence and approximate level of sewage contamination.

1. Introduction

Water pollution has been a major challenge to the global sustainable development. The sources of fresh or potable water, such as groundwater, are becoming scarce due to much higher rates of anthropogenic depletion than the rate of natural recharge [1–4]. The human population living under water scarcity has increased from around 14% of global population to around 58% of global population in the 2000s [5]. Moreover, many fresh water sources are becoming increasingly polluted and require increasing treatment to be suitable for drinking and cooking [6–10].

In many areas simple field tests could be valuable to determine the quality of a water for potable use, for example with respect to ground water resources. This is even more important if the reclaimed water is targeted for recharging tanks, wells and groundwater in arid geographical areas and remote human settlements where water scarcity and/or lack of water treatment plants forces the local population to depend on

any available water source [11]. In remote areas, access to a simple pollution indicator test could be a valuable tool to improve water safety. Such tests could also be used to check efficiency of water treatment systems that are in place. Simple field-friendly water quality tests to determine inflow of wastewater discharge into rivers in the field could also be useful to determine if combined sewer overflows near urban areas are spilling at a higher frequency than permitted [12]. Likewise simple water quality indicator tests could be useful for emergency responses in natural disaster areas where there can be an acute need to indicate cross contamination between wastewater and potable water resources [13]. Moreover, there are a number of factors or incidents which can cause an unintended ingress of municipal wastewater into a natural water body, including sanitary sewer overflows, and misconnections in separate sewer systems where home appliances are mistakenly connected to the storm sewer rather than to the sanitary sewer [14,15]. The misconnections put a significant pollutant load onto natural water bodies [15]. These are usually infrequent and localised events and the *in situ*

* Corresponding author. Department of Chemical and Biological Engineering, University of Sheffield, Sheffield, S1 3JD, UK.

** Corresponding author.

E-mail addresses: s.ebbens@sheffield.ac.uk (S.J. Ebbens), xiubo.zhao@sheffield.ac.uk (X. Zhao).

pollutant detection is therefore difficult to conduct. The detection methods rely on a number of marker compounds that would only be present in household discharge. These markers can be either chemical or biological and vary in difficulty of detection, with only a few being detectable rapidly and *in situ* [14,16–18].

Current available field methods for direct assessment of water quality often rely on chemical sensors which require a source of power and are relatively costly in procurement. Alternatively, samples are collected and sent to the laboratory for direct detection of soluble pollutants, requiring sophisticated laboratory equipment [19]. However, here we investigate utilising the surface tension reductions that are signatures of some important sources of water contamination, as an approach that enables cheap and responsive monitoring. Specifically, we consider the case of detecting water contaminated with wastewater, and show that surface tension reduction provides a good indicator of the level of contamination. Sewage wastewater is a complex mixture of water, containing particulate matter, micro-organisms and pollutants, such as heavy metals, micro-plastics and detergents [20]. The resulting presence of these solutes, surfactants and other miscible compounds affects the surface tension of the liquid depending on their surface excess or surface concentration [21–23]. Indeed, the relationship between surface tension and water borne pollution is well established, and surface tension criteria have consequently been used for environmental water monitoring [24]. A rapid *in situ* detection of surface tension could therefore be an important first indicator in situations where wastewater contamination is possible. This detection method would also be valuable in the misconnection scenario described above, where surface tension lowering detergents are indicative of faults. Such tests will be also be useful for screening drinking water supplies in rural, remote and arid areas and in those urban areas where there is a limit of resources, such as, laboratory facilities, skilled manpower and ample amount of time, or where a quick response is important [25].

In this context, here, we have devised printable surface tension gradient driven self-propelling sensors with millimetre-scale dimensions whose motion properties reflect surface tension values, and thus, can act as an indicator for certain contaminants in water samples, allowing for simple rapid initial indication of water quality in the field, to direct further tests or investigations. The silk fibroin sensors, that we investigate here for this application, continuously leach a soluble surface-active compound, poly (ethylene glycol) (MW = 400) (PEG₄₀₀), to create a surface tension gradient. This causes motion at the air-water interface via the Marangoni effect [26]. In previous studies by Zhang et al. [26] and Gregory et al. [27], it has been demonstrated that it is possible to control the propulsion behaviour of these, and other related devices, by varying their composition and structure during manufacture via reactive inkjet printing. It was also described that the propulsion behaviour of the Marangoni effect driven stirrers propelling in varying concentrations of an aqueous anionic surfactant, sodium dodecyl sulphate (SDS), correlated with the solutions' surface tension. Specifically, the stirrers' number of revolutions per minute (RPM) during rotational propulsion was found to decrease as the concentration of SDS increased from 0.3 mM to 1.0 mM [26]. The aim of the present work is to determine whether this propulsion system can consequently be utilised to distinguish between wastewater samples of different surface tensions, with sufficient resolution so that it can indicate their quality differences by, ideally, only requiring observation of the sensors' motion by eye without any further complicated analysis of propulsion behaviour.

2. Experimental methods

2.1. Materials

Bombyx mori silkworm cocoons were obtained from State Key Laboratory of Silkworm Genome Biology and Biological Science Research Centre, Southwest University, China. Silicon wafer substrates for printing 3D structures were purchased from Compact Technology Ltd, UK.

Ultrapure high quality deionized water (DI water), filtered with 0.2 µm filter, was used in all experiments. All other chemicals were commercially obtained and were of analytical grade. Sodium carbonate (Na₂CO₃) was purchased from Alfa Aesar. Calcium chloride (CaCl₂) was purchased from Fluka Analytical. Ethanol (C₂H₅OH) was purchased from Fisher Scientific. Methanol (CH₃OH) was purchased from Acros Organics. PEG₄₀₀ and cellulose derived dialysis tubes with molecular weight cut-off of 12 kDa–14 kDa were purchased from Sigma Aldrich.

2.2. Collection of wastewater

Urban wastewater (WW) containing a mixture of domestic and industrial wastewater was used in the experiments as it is a highly contaminated source of water and can be diluted down to represent any natural and artificial water source, such as rivers, ponds and urban supply water. The wastewater was inlet wastewater collected from a sewage treatment plant (Woodhouse Mills Wastewater Treatment Plant in Sheffield, UK) after it had been passed through coarse and fine screening to remove large debris and grit, but before any chemical or biological treatment had been done. The sewage was collected in 500 mL bottles and stored at 2 °C for use in the experiments.

2.3. Wastewater sample preparation

The collected wastewater was diluted down to four different concentrations of 10%, 5%, 3% and 1% for the experiments by adding different amounts of deionized water. In addition, 100% pure deionized water (henceforth called wastewater-0% or WW-0%) was also used for comparison and to understand how soluble contaminants affect water's physical properties in terms of its chemical oxygen demand and surface tension.

2.4. Characterization of wastewater: chemical oxygen demand

The chemical oxygen demand of wastewater samples was measured by the COD cuvette test (LCK 514, Hach Lange Ltd, UK) using a COD spectrophotometer (Hach Lange Ltd, UK). For each reading, 2 mL of the wastewater samples were used in each analysis following the manufacturer's instructions. A reaction with 2 mL of deionized water was used as blank. The cuvettes were then heated to 148 °C for 2 h in a thermostat. The spectrophotometer was calibrated using COD standards with concentrations of 0, 100, 200, 300 and 400 mg/L COD.

2.5. Characterization of wastewater: surface tension

The surface tensions of the different wastewater samples were measured by a tensiometer (K11 MK4, KRÜSS GmbH, Germany) with a standard platinum plate probe measuring 19.9 × 10 × 0.2 mm in dimensions and having an immersion depth of 2 mm in the sample. Five measurements were taken for each WW sample to obtain the mean values along with their standard deviation of mean. 10 mL of sample was taken for each measurement conducted at an ambient temperature of around 20 °C. Each measurement was run for 50 min generating 3000 readings, of which, the last 10 readings were averaged automatically by the tensiometer to give the final reading of the surface tension of the sample.

2.6. Sensor fabrication by 3D inkjet printing

The water quality detecting sensors were fabricated in a shape similar to the letter 'Z' using an in-house built 3D inkjet printer fitted with piezoelectric jetting devices (MicroFab Technologies, USA). The specific shape was chosen to keep this work consistent with our previous work [26] where we have observed that such a 'Z'-like shape encourages rotation or circular motion to be the dominant form of propulsion pattern, thus making the tracking and calculation of velocities easier. The propelling sensors were fabricated from regenerated silk fibroin (RSF)

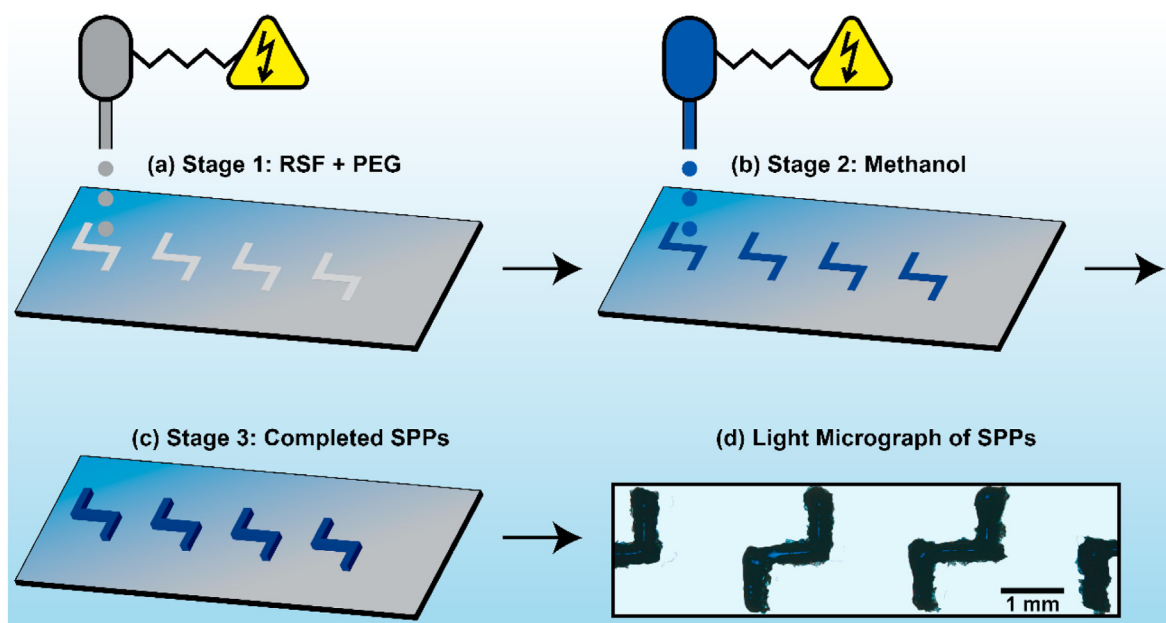


Fig. 1. Schematic illustration of the layer-by-layer process of reactive inkjet (RIJ) printing of Z-shaped sensors from regenerated silk fibroin (RSF)/PEG₄₀₀ (primary ink) and methanol (curing ink). **(a)** Stage 1 is the deposition of the primary ink to form the body of the indicators. **(b)** Stage 2 is the deposition of the curing ink to transform the soluble random coil proteins of silk fibroin into the insoluble β -sheet structure. Additionally, this stage provides visibility to the otherwise transparent sensors due to the deposition of Coomassie brilliant blue dye mixed in the curing ink. **(c)** Stage 3 is the final fabricated 3D structures formed after 150 consecutive repetitions of the stages 1 and 2. **(d)** Image-adjusted light micrograph of a section of the silicon wafer with freshly printed sensors. (For interpretation of the references to colour in this figure legend, the reader is referred to the Web version of this article.)

solution, which was prepared using the previously described procedure [27]. In this study, the concentrations of RSF and PEG₄₀₀ were kept at 40 mg/mL and 20 mg/mL, respectively. The raw materials, RSF and PEG₄₀₀ used for fabrication, are easily accessible and safe to use, thereby keeping the cost of fabrication minimal and having no risk of environmental hazard. PEG₄₀₀ acts as the fuel to propel the sensors as it leaches out from them into the water, thus, causing a local decrease in the surface tension which causes propulsion due to the Marangoni effect [26,27]. During fabrication, 150 layers of primary ink was printed on a silicon wafer substrate to yield one batch of Z-shaped sensors. Each layer of the primary ink was cured with a layer of methanol mixed with Coomassie brilliant blue dye to provide contrasting blue colour to the sensors for better visibility. The dimensions of the mid-section and the two arms of the Z-shaped sensors were, respectively, set to be approximately 2.0 mm and 0.5 mm. Fig. 1 schematically illustrates the process of RIJ printing alongside a representative light micrograph of a freshly printed sensors.

2.7. Sensor propulsion in wastewater

After the printing, the individual sensors were taken off from the silicon wafer substrate very carefully using a fine needle, making sure that no physical damage or distortion occurs. The PEG₄₀₀-doped sensors were then placed on the surface of deionized water having a conductivity of $<1 \mu\text{S}/\text{cm}$ (wastewater-0% or WW-0%) and the four previously diluted concentrations of the sewage wastewater (WW-1%, WW-3%, WW-5%, and WW-10%) for the propulsion test. Each printed sensor was used for a single propulsion test after which it was discarded. This was repeated 5 times for each of the wastewater concentrations. For each experiment, 4 mL of the appropriate liquid sample was placed in a 3 cm diameter well of a 12-well plate which is lit up with a white LED light source (AGPtek Lightpad). The sensor propulsion was video-recorded at 100 frames per second (fps) for 60 s, totalling to 6000 frames, using a PixeLink™ CCD colour camera [model: PL-D732CU-T] fitted with Navitar™ macro zoom lens [model: 1-60135 zoom tube lens with 1-6010 camera coupler attachment]. After recording, ImageJ was used to generate image sequence from the video frames for all the sensors.

2.8. Propulsion trajectory tracking and analysis

Automatic tracking of the sensors was done as previously described [27]. Briefly, the propulsion trajectory was tracked using an in-house built tracking programme based on LabVIEW™ (National Instruments Corporation, USA). After importing the video in the tracking software, the two edges of a sensor were pinpointed for tracking and were traced throughout the video frame-by-frame to generate the propulsion path of the sensor. The software also calculated the instantaneous velocities (v_{inst}) at the edges and the centres of each of the sensors in each frame, which were analysed for determining the rate of decay of propulsion velocity of a sensor over the observation time of 60 s. The v_{inst} was obtained as micrometres per second for each of the frame, thus, totalling to 6000 data points, which were then smoothed by adjacent averaging in OriginPro™ and plotted as velocity–time graph to observe v_{inst} decay over the 60-s period.

2.9. Statistics

The instantaneous velocities of the propelling sensors were generated once every 0.01 s, which was the time gap between two consecutive video frames. This gave a total of 6000 data points for instantaneous velocity for a 60 s long video. These instantaneous velocities were then plotted against time (t) to generate the instantaneous velocity decay curve of each sensor. Next, the time taken by the sensors to reach half and quarter of their initial instantaneous velocities was calculated and averaged for all the samples for plotting as a bar chart along with respective standard deviation of mean. All the graphs and the data from measurements of chemical oxygen demand and surface tension were plotted in Origin™.

3. Results

It is important to first analyse the wastewater used in this experiment, to ensure transferability and generality of our results. For this, the chemical oxygen demand (COD), a measure of the organic matter

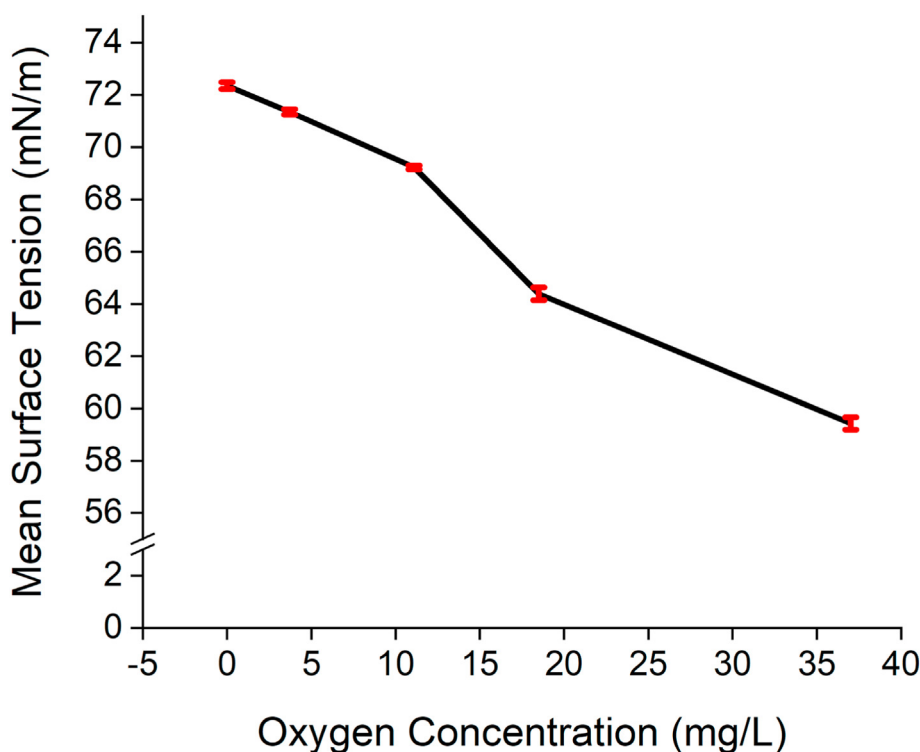


Fig. 2. Correlation between the amount of contaminant, measured as Chemical Oxygen Demand (COD), and surface tension of different dilutions of the wastewater. COD was estimated from the absorbance values measured in absorbance units (au) in a spectrophotometer. The oxygen concentrations of WW-0%, WW-1%, WW-3%, WW-5% and WW-10% were measured to be 0, 3.7, 11.1, 18.5 and 37 mg/L, respectively, and their mean surface tension values were measured to be 72.35, 71.34, 69.22, 64.38 and 59.42 mN/m, respectively. Standard deviation of mean is shown as error bars in red. (For interpretation of the references to colour in this figure legend, the reader is referred to the Web version of this article.)

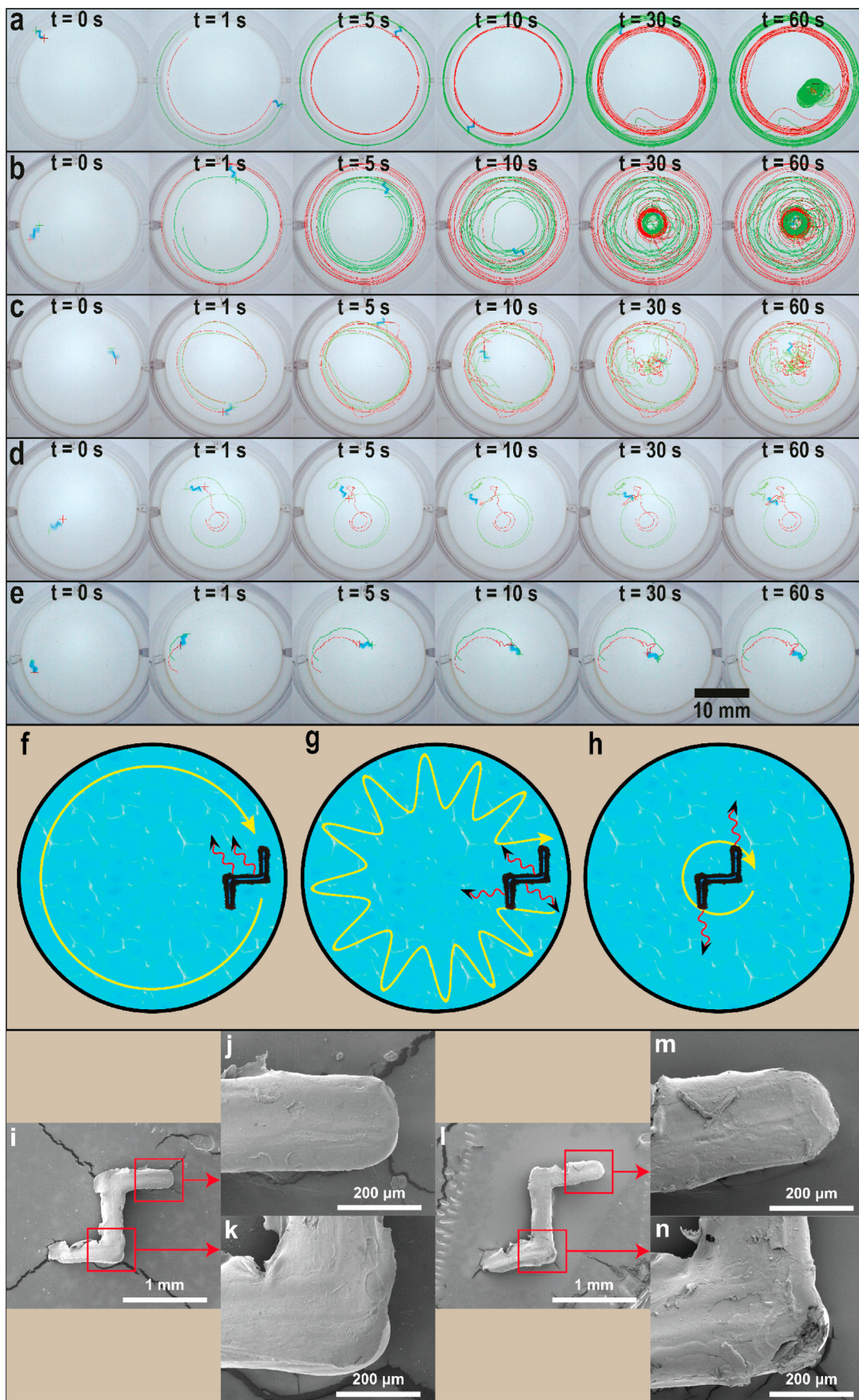
content, of the collected wastewater was used. Triplicate samples were analysed for COD and the average was 370 ± 6 mg/L. This COD is relatively low for this wastewater treatment works, where more typical dry weather COD values would be between 600 and 700 mg/L, indicating a slight rain impact on the samples, but still a significant content of domestic wastewater in the samples. The wastewater samples used in the surface tension experiments was diluted to contain, 0%, 1%, 3%, 5% and 10% of this wastewater meaning that the samples would have had the COD values of 0, 3.7, 11.1, 18.5 and 37 mg/L, respectively.

Next, it was checked if the level of wastewater in the samples corresponds to a change in surface tension, which is the key link required to enable our proposed sensing method. Fig. 2 shows the surface tension (ST) values of the 5 different water samples calculated using a tensiometer (KRÜSS GmbH), plotted against COD presented as oxygen concentration. The ST values of the wastewater diluted to the concentrations of 0%, 1%, 3%, 5%, and 10%, respectively, are 72.4 ± 0.14 , 71.3 ± 0.11 , 69.2 ± 0.07 , 64.4 ± 0.25 , and 59.4 ± 0.24 mN/m (here, 0% means deionized or pure water). In contrast, the surface tension of the collected wastewater sample before any dilution was found to be ~ 35 mN/m. An approximately linear reduction in surface tension is observed over this range as a function of COD, establishing the required link between the level of contamination in the samples and surface tension.

Having established this link, we proceeded to investigate the motion of the propelling sensors in each wastewater dilution. Fig. 3 (a – e) shows the selected time sequence frames of propulsion trajectory of one representative sensor from each wastewater concentration. In contrast, no movement at all was observed in sensors placed in the original collected wastewater sample, which had a surface tension of ~ 35 mN/m. After observing all the propulsion behaviours from all wastewater samples, we have systematised and classified the propulsion behaviour of the sensors into three main patterns, which are revolution, zig-zag and rotation as illustrated in Fig. 3 (f – h). We define these patterns as follows: (1) Revolution is the smooth circular motion of a sensor along the periphery and around the centre of the well; (2) Zig-zag is the to-and-fro motion of a sensor between the central region and the periphery with an overall circular motion around the centre of the well; (3) Rotation is

the circular motion of a sensor roughly around its own centre of axis. For the WW-0% sample, the propulsion trajectory clearly followed one or more of the three main patterns as shown in Fig. 3 (a). In addition, the motion remained smoothly decelerating throughout the 60 s of the observation period. On increasing wastewater concentration, even though the three motion patterns were observed, the propulsion deceleration became less and less smooth, such as in Fig. 3 (c – d). As the wastewater concentration is increased even further, the three patterns became less evident, with the sensor propelling in WW-10% moving only with a momentary jerk and coming to an almost halt in less than 5 s in all samples. These differences in the observed sensor propulsion patterns suggest that the decreased surface tension confirmed for higher concentration wastewater samples may be disrupting the Marangoni effect driven motion, and decrease the time up to which the sensor can keep propelling. This is in line with the previous reports of loss of rotation rate as surface tension was reduced in simple water-surfactant solutions [26, 27]. However, without further analysis, it is not possible to unambiguously link all the observed motion changes with surface tension, as other chemical compositional changes or changes in the sample's fluid properties may also interfere with propulsion, albeit to a lesser degree. Fig. 3 (i – n) shows the SEM images of a sensor before and after propulsion with little morphological difference observed in the magnified images, similar to a previous study [26]. This suggests that the rigid structure of the sensor is porous enough to allow PEG₄₀₀ molecules to simply diffuse out without causing excessive micrometre-scale structural changes or damages to the sensor morphology.

The time of occurrence and duration of a specific pattern of motion could not be successfully predicted. Thus, it can be said that the type of sensor propulsion pattern is not indicative of the water quality or the contaminant concentration and the resultant surface tension. This makes it difficult to estimate the surface tension or contaminant level of the given water sample just by visually observing a sensor's propulsion pattern. However, both quantitative and qualitative consistent changes in motion can still be distinguished, regardless of the overall pattern of motion. *A priori* it seemed a reasonable expectation that the initial instantaneous velocity would reduce with surface tension/contamination



(caption on next page)

Fig. 3. Time sequence of sensors with PEG₄₀₀ propelling in wastewater samples at concentrations (v/v %) of (a) 0% (b) 1% (c) 3% (d) 5% (e) 10%. One small blue coloured sensor can be seen propelling in each well, with the propulsion trajectory marked by red and green coloured lines positioned at the two edges of each sensor. (f–h) Illustration of the three main types of propulsion behaviour shown by the surface-tension-driven sensors. The red-black arrows indicate supposed direction of leaching of PEG₄₀₀. (f) Revolution along the periphery of the well; (g) Zig-zag or see-saw motion between centre and periphery of the well; (h) Rotation along its own centre of mass. (i–n) SEM images of the sensors (i) before propulsion, (j–k) with magnification; (l) after propulsion, (m–n) with magnification. The post-propulsion SEM images show mild erosion of the surface topography. (For interpretation of the references to colour in this figure legend, the reader is referred to the Web version of this article.)

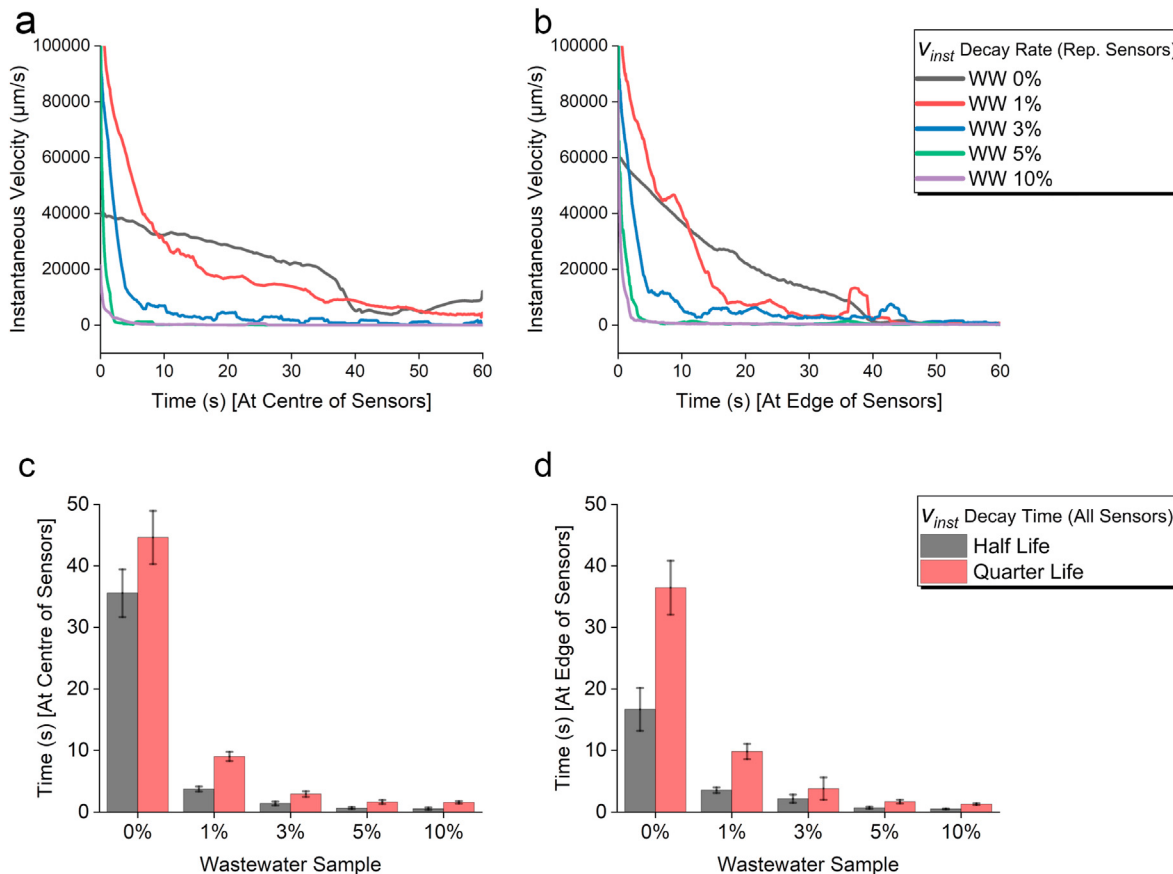


Fig. 4. (a–b) Instantaneous velocity (v_{inst}) decay rates of one representative sensor over a period of 60 s (a = centre, b = edge). Each line in the graphs is taken from the one representative sensor which has its v_{inst} half-life and quarter-life values closest to the mean half-life and mean quarter-life values shown in the bar graphs in ‘c’ and ‘d’. (c–d) Mean instantaneous velocity (mean v_{inst}) decay times of all PEG₄₀₀ containing sensors propelling in different wastewater samples (c = centre, d = edge). The decay is assessed as the time taken for the mean v_{inst} to reach half and quarter of its initial value. The error bars are measured from the v_{inst} decay time data of 5 sensors for each water sample.

level, and provide a useful metric. This was based on the expectation that the initial motion was driven by the surface tension difference between PEG₄₀₀ and the fluid surface the stirrer was placed onto, and wastewater would reduce this difference. However, Fig. 4 (a – b) shows that the initial velocities for sensors in contaminated samples, can actually significantly exceed those for pure water. The origin of this effect is not fully understood and could reflect modifications to other unreported fluid properties such as viscosity, or changes in the stirrers caused by components of the complex mixture. However, despite this unexpected finding, the rate of decay of velocity of the sensors was found to instead be a useful metric, as described below.

Fig. 4 (a – b) shows the instantaneous velocity (v_{inst}) decay rates of one representative sensor propelling in each of the 5 wastewater concentration samples. Fig. 4 (a) shows the data obtained by tracking the centre of the sensors whereas Fig. 4 (b) shows the data obtained by tracking one of the edges of the sensors. The v_{inst} values are plotted as line graph against time, thereby showing their gradual deceleration or decay over time. Similar with the half-life and quarter-life data, the representative v_{inst} decay rates also show significant differences among the v_{inst} of sensors

propelling in WW-0%, WW-1% and WW-3% but not between WW-5% and WW-10%. Similarity between the data obtained by tracking the centre and the data obtained by tracking the edge of the stirrers shows the consistency of results and confirms the accuracy of the measurements. One important feature to notice is that the v_{inst} decay rate is not dependant on the initial velocity of the sensors. For instance, as remarked on above, the initial velocity of the sensors in WW-0% is much less in comparison to those of the sensors in WW-1% and WW-3%. However, the decay rate of v_{inst} is much lower for the sensors propelling in WW-0% than the sensors propelling in all other samples. Selected video frames of the representative sensors are also depicted as image sequences in Fig. 3 (a – e). The frame-by-frame v_{inst} data is used to determine how much time the sensors take to reduce to half and quarter values of their initial propulsion velocities. Fig. 4 (c – d) shows the mean times taken by the sensors (sample size = 5) to reach the half and quarter values of their initial velocities. Fig. 4 (c) shows the data obtained by tracking the centre of the sensors whereas Fig. 4 (d) shows the data obtained by tracking one of the edges of the sensors. The mean values are plotted as bar graph with error bars representing the respective standard deviation of mean of the

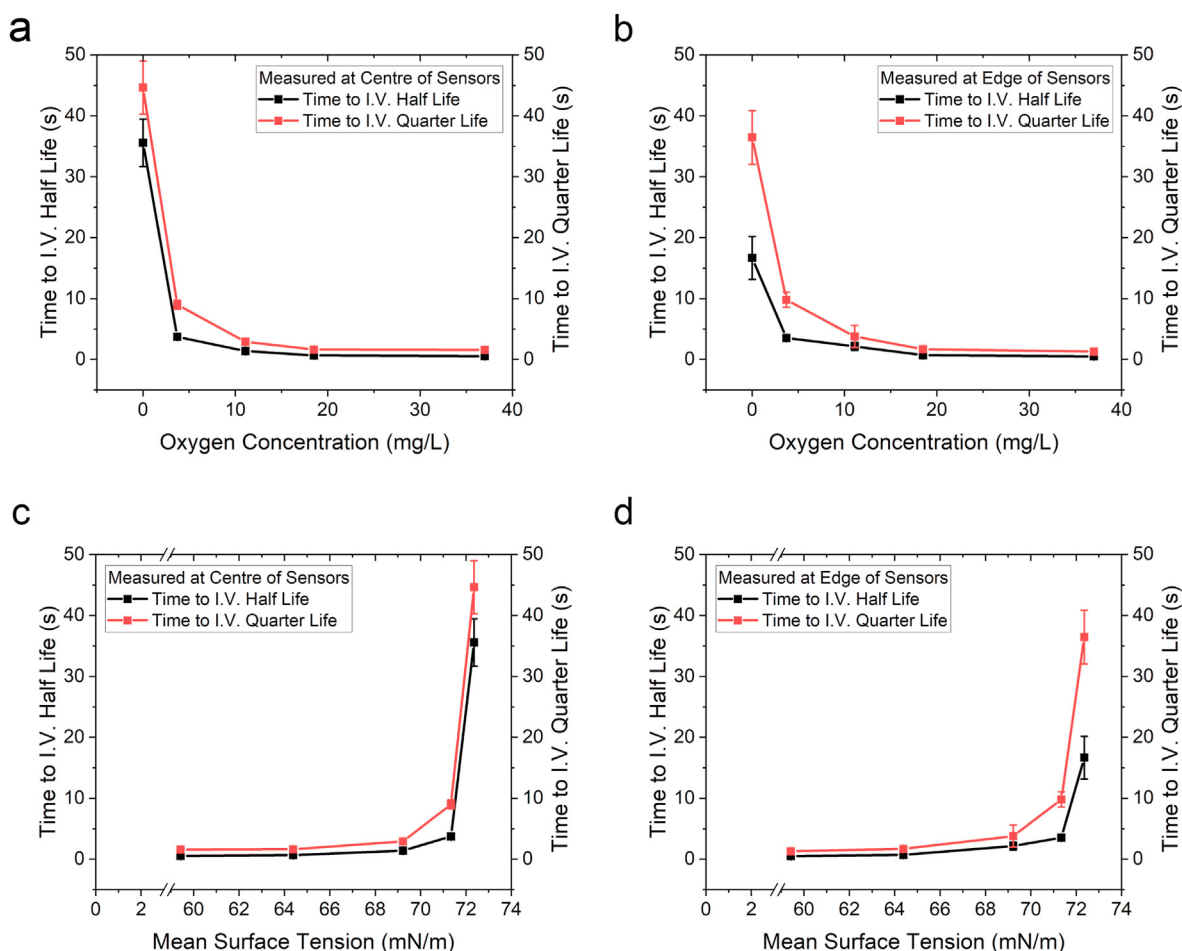


Fig. 5. (a–b) Mean initial velocity half-life and quarter-life of the sensors as measured against the contaminant concentration which is represented by the oxygen concentration values (calculated from the chemical oxygen demand) taken from different wastewater samples (a = centre, b = edge). (c–d) Mean initial velocity half-life and quarter-life of the sensors as measured against the surface tension values taken from different wastewater samples (c = centre, d = edge).

data from five sensors for each water sample. The data in the graphs show that there are significant differences between the v_{inst} decay half-life and quarter-life of the sensors propelling in WW-0%, WW-1% and WW-3%. The difference, however, becomes insignificant between WW-5% and WW-10%, suggesting that the technique employed in this study is readily applicable to detecting very low levels of impurities, which cause very little difference in surface tension values. This reflects the high sensitivity of the propulsion mechanism to surface tension.

Note that also, during the sensor propulsion, the v_{inst} decay rates show minor deviations in the form of minute crests and troughs as can be seen in the line graphs in Fig. 4 (a – b). In the primary ink, silk fibroin and PEG₄₀₀ are completely miscible with each other which makes the primary ink a very homogeneous mixture. However, as the printed structures were at millimetre-scale, the formation of the rigid and insoluble silk fibroin β -sheets within the sensors remains uneven at molecular level. This causes an uneven distribution of PEG₄₀₀ throughout the three-dimensional structure of the sensors as they get fabricated layer-by-layer during RIJ printing, leading to an unpredictable rate and direction of leaching of PEG₄₀₀ out of different regions of the sensor at the air-water interface, that could account for these variations, and explain the different motion patterns described above. Similar observation have also been reported in other studies using silk fibroin–PEG₄₀₀ sensors [26] and water soluble camphor [28–30] propelling at the air-water interface through the Marangoni effect.

Double-Y axes graphs were plotted, as shown in Fig. 5, in order to observe a clearer correlation between the contaminant concentration (represented by COD/oxygen concentration) and sensor velocity decays

and between the surface tension values and sensor velocity decays. Fig. 5 (a – b) shows the link between the oxygen concentration and the time it takes for the mean velocities (I.V.) of the sensors to reach half and quarter of their respective initial values. Similarly, Fig. 5 (c – d) shows the link between the surface tension values and the time it takes for the mean velocities (I.V.) of the sensors to reach half and quarter of their respective initial values. It can be observed that a very small concentration of contaminant is able to drastically increase the deceleration rate of sensor propulsion velocity across all samples. The propulsion velocity of the sensors reduced to almost 0 when the concentration of the oxygen increased to 20 mg/L, indicating that the sensors are super sensitive to the trace of contamination in water. In the meanwhile, the propulsion velocity decreased remarkably when the surface tension reduced from 72 mN/m (clean water) to 69 mN/m, also indicating the excellent sensitivity to the change of water surface tension, which is an important parameter for clean water.

4. Discussion

Having concluded that the instantaneous velocity decay is the best way to tell the difference between water samples irrespective of which of the 3 main propulsion patterns occurs, we consider potential practical deployments of the sensors for testing. In this regard, the best readout method was to use a timer and observe the total propulsion time or the time the sensor takes to reach a halt, which as explained earlier, was notably different among the different concentrations of the wastewater sample. From there, the surface tension of a wastewater sample could be

roughly estimated. As well as altering the surface tension gradients that drive the sensors, the surface tension of the surrounding fluid at a given point in time will also determine the meniscus wetting effects at the surface of the stirring device. This is an additional mechanism that can contribute to the observed velocity profiles. For example, wetting changes will alter the surface area of the device that is in contact with the fluid, which could in turn modify fluid drag, and also PEG leaching rate. As the ultimate objective of this study was to be able to visually distinguish the differences in propulsion behaviour in order to readily diagnose a water sample, it was important to focus on those results which significantly differ from each other (WW-0% vs. all other, WW-1% vs. all other, WW-3% vs. all other) instead of those which marginally or insignificantly differ from each other (WW-5% vs. WW-10%). On visual inspection of the sensor propulsion, it could be deduced that between the 0% and 5% samples or 1% and 10% samples the difference in propulsion velocity and v_{inst} decay times were significant enough to be detectable and viably discernible by human eye. This difference was found to be too subtle between the 3% and 5% or 5% and 10% samples to be detectable by eye. For that, in the future, an image analysis-based detection system could be developed which could use a mobile phone's camera to continuously scan and capture the sensor propulsion on the field and match it online against a video library of calibrated sensor propulsion data to roughly estimate the surface tension and, thus, obtain the miscible waste or contaminant concentration values in a water sample. Thus, a better resolution in this quantitative analysis-based approach could be envisaged. Afterwards, if a sample is found to contain a large amount of contaminants, then it can be sent from the field to a laboratory for further investigation so that the water sample source can be treated to prevent widespread contamination. Moreover, while this work reports on the ability to infer water quality by sensing surface tension, we have also shown elsewhere [27, 31] that propulsion can be generated via enzymatic reactions. As enzymatic reactions are inhibited by particular chemical agents, it is possible that future work could exploit equivalent enzymatically driven motion sensors to detect specific contaminants.

The fact that this technique was able to assess very low concentrations of pollutants makes it a very attractive technique because it could be seen that sensor propulsion behaviour shows marked difference between WW-0%, WW-1% and WW-3% whereas the tensiometer data may not be sensitive enough at such small differences in the miscible contaminant or impurity levels. The wastewater sample we used is typical of the sewage contamination that could be expected in the UK, and beyond, and so the reported effectiveness suggests wide potential. Furthermore, it is clear that misconnections that often lead to detergent entering storm drains in separate sewer systems are likely to be highly amenable to detection through surface tension, making our sensors potentially impactful in this context as well.

5. Conclusion

In this study, we successfully produced self-propelling millimetre-sized sensors via dynamic alteration of the surface tension gradient at the air-water interface. We also demonstrated that the propulsion behaviour of the printable sensors was strongly dependent on wastewater contaminant concentration, which in turn can act as a diagnostic tool for the assessment of a given water sample. The decay rate, half-life, and quarter-life of the sensors' instantaneous velocities in different samples showed a strong correlation to the wastewater content, discernible via simple visual inspection, and can be further augmented by, for example, smart phone-based motion analysis in the future.

CRedit author statement

Piyush Kumar: Conceptualization, Methodology, Software, Validation, Formal analysis, Investigation, Data curation, Writing - Original Draft, Writing - Review & Editing, Visualization. **Abigail Legge:** Methodology. **David Gregory:** Methodology, Software, Data Curation. **Andy**

Nichols: Conceptualization. **Henriette Jensen:** Conceptualization, Methodology, Formal analysis, Investigation. **Stephen Ebbens:** Conceptualization, Methodology, Software, Validation, Formal analysis, Resources, Writing - Review & Editing, Supervision, Funding acquisition. **Xiubo Zhao:** Conceptualization, Methodology, Validation, Resources, Writing - Review & Editing, Supervision, Project administration, Funding acquisition.

Declaration of competing interest

The authors declare no conflict of interest.

Acknowledgements

The authors would like to acknowledge the EPSRC (EP/N007174/1, EP/N023579/1, EP/J002402/1, and EP/N033736/1) for support. The authors also thank Mr. Mick Fletcher and Woodhouse Mills Wastewater Treatment Plant, Sheffield, UK for providing us with wastewater samples.

Appendix A. Supplementary data

Supplementary data to this article can be found online at <https://doi.org/10.1016/j.jciso.2022.100044>.

References

- [1] J.J. Gurdak, Climate-induced pumping, *Nat. Geosci.* 10 (2) (2017) 71, 71.
- [2] J.S. Famiglietti, The global groundwater crisis, *Nat. Clim. Change* 4 (11) (2014) 945–948.
- [3] B. Ashraf, A. AghaKouchak, A. Alizadeh, M. Mousavi Baygi, H.R. Moftakhari, A. Mirchi, H. Anjileli, K. Madani, Quantifying anthropogenic stress on groundwater resources, *Sci. Rep.* 7 (1) (2017) 12910.
- [4] V. Srinivasan, E.F. Lambin, S.M. Gorelick, B.H. Thompson, S. Rozelle, The nature and causes of the global water crisis: syndromes from a meta-analysis of coupled human-water studies, *Water Resour. Res.* 48 (10) (2012).
- [5] M. Kumm, J.H.A. Guillaume, H. de Moel, S. Eisner, M. Flörke, M. Porkka, S. Siebert, T.I.E. Veldkamp, P.J. Ward, The world's road to water scarcity: shortage and stress in the 20th century and pathways towards sustainability, *Sci. Rep.* 6 (1) (2016) 38495.
- [6] Z. Xu, J. Xu, H. Yin, W. Jin, H. Li, Z. He, Urban river pollution control in developing countries, *Nat. Sustain.* 2 (3) (2019) 158–160.
- [7] Y. Wen, G. Schoups, N. van de Giesen, Organic pollution of rivers: combined threats of urbanization, livestock farming and global climate change, *Sci. Rep.* 7 (1) (2017) 43289.
- [8] H.-M. Chen, M.-T. Wu, Residential exposure to chlorinated hydrocarbons from groundwater contamination and the impairment of renal function-An ecological study, *Sci. Rep.* 7 (1) (2017) 40283.
- [9] P. Höhener, D. Werner, C. Balsiger, G. Pasteris, Worldwide occurrence and fate of chlorofluorocarbons in groundwater, *Crit. Rev. Environ. Sci. Technol.* 33 (1) (2003) 1–29.
- [10] T. Kistemann, J. Hundhausen, S. Herbst, T. Claßen, H. Färber, Assessment of a groundwater contamination with vinyl chloride (VC) and precursor volatile organic compounds (VOC) by use of a geographical information system (GIS), *Int. J. Hyg. Environ. Health* 211 (3) (2008) 308–317.
- [11] L.A. Schaidler, K.M. Rodgers, R.A. Rudel, Review of organic wastewater compound concentrations and removal in onsite wastewater treatment systems, *Environ. Sci. Technol.* 51 (13) (2017) 7304–7317.
- [12] Z. Wang, D. Shao, P. Westerhoff, Wastewater discharge impact on drinking water sources along the Yangtze River (China), *Sci. Total Environ.* 599–600 (2017) 1399–1407.
- [13] I. Keenum, M.C. Medina, E. Garner, K.J. Pieper, M.F. Blair, E. Milligan, A. Pruden, G. Ramirez-Toro, W.J. Rhoads, Source-to-Tap assessment of microbiological water quality in small rural drinking water systems in Puerto Rico six months after hurricane maria, *Environ. Sci. Technol.* 55 (6) (2021) 3775–3785.
- [14] N.H. Tran, M. Reinhard, E. Khan, H. Chen, V.T. Nguyen, Y. Li, S.G. Goh, Q.B. Nguyen, N. Saeidi, K.Y.-H. Gin, Emerging contaminants in wastewater, stormwater runoff, and surface water: application as chemical markers for diffuse sources, *Sci. Total Environ.* 676 (2019) 252–267.
- [15] D.M. Revitt, J.B. Ellis, Urban surface water pollution problems arising from misconnections, *Sci. Total Environ.* 551–552 (2016) 163–174.
- [16] H. Yin, M. Xie, L. Zhang, J. Huang, Z. Xu, H. Li, R. Jiang, R. Wang, X. Zeng, Identification of sewage markers to indicate sources of contamination: low cost options for misconnected non-stormwater source tracking in stormwater systems, *Sci. Total Environ.* 648 (2019) 125–134.
- [17] Y.O.O. Hu, N. Ndegwa, J. Alneberg, S. Johansson, J.B. Logue, M. Huss, M. Källér, J. Lundeberg, J. Fagerberg, A.F. Andersson, Stationary and portable sequencing-based approaches for tracing wastewater contamination in urban stormwater systems, *Sci. Rep.* 8 (1) (2018) 11907.

- [18] D.M. Chandler, D.N. Lerner, A low cost method to detect polluted surface water outfalls and misconnected drainage, *Water Environ. J.* 29 (2) (2015) 202–206.
- [19] F. Robert-Peillard, A.D. Syakti, B. Coulomb, P. Doumenq, L. Malleret, L. Asia, J.L. Boudenne, Occurrence and fate of selected surfactants in seawater at the outfall of the Marseille urban sewerage system, *Int. J. Environ. Sci. Technol.* 12 (5) (2015) 1527–1538.
- [20] C. Warwick, A. Guerreiro, A. Soares, Sensing and analysis of soluble phosphates in environmental samples: a review, *Biosens. Bioelectron.* 41 (2013) 1–11.
- [21] L. Martínez-Balbuena, A. Arteaga-Jiménez, E. Hernández-Zapata, C. Márquez-Beltrán, Applicability of the Gibbs Adsorption Isotherm to the analysis of experimental surface-tension data for ionic and nonionic surfactants, *Adv. Colloid Interface Sci.* 247 (2017) 178–184.
- [22] C. Wang, X. Wang, F. Liu, Z. Jiang, X. Lin, Surface concentration or surface excess, which one dominates the surface tension of multicomponent mixtures? *Colloid Polym. Sci.* 296 (1) (2018) 89–93.
- [23] A. Mitropoulos, What is a surface excess? *J. Eng. Sci. Technol. Rev.* 1 (2008).
- [24] M.K.C. Sridhar, C. Rami Reddy, Surface tension of polluted waters and treated wastewater, *Environmental Pollution Series B, Chem. Phys.* 7 (1) (1984) 49–69.
- [25] K.S. Manja, M.S. Maurya, K.M. Rao, A simple field test for the detection of faecal pollution in drinking water, *Bull. World Health Organ.* 60 (5) (1982) 797–801.
- [26] Y. Zhang, D.A. Gregory, Y. Zhang, P.J. Smith, S.J. Ebbens, X. Zhao, Reactive inkjet printing of functional silk stirrers for enhanced mixing and sensing, *Small* 15 (1) (2019), e1804213.
- [27] D.A. Gregory, P. Kumar, A. Jimenez-Franco, Y. Zhang, Y. Zhang, S.J. Ebbens, X.B. Zhao, Reactive inkjet printing and propulsion analysis of silk-based self-propelled micro-stirrers, *Jove-J. Vis. Exp.* 146 (2019).
- [28] N.J. Suematsu, T. Sasaki, S. Nakata, H. Kitahata, Quantitative estimation of the parameters for self-motion driven by difference in surface tension, *Langmuir* 30 (27) (2014) 8101–8108.
- [29] S. Nakata, M. Murakami, Self-motion of a camphor disk on an aqueous phase depending on the alkyl chain length of sulfate surfactants, *Langmuir* 26 (4) (2010) 2414–2417.
- [30] N.J. Suematsu, Y. Ikura, M. Nagayama, H. Kitahata, N. Kawagishi, M. Murakami, S. Nakata, Mode-switching of the self-motion of a camphor boat depending on the diffusion distance of camphor molecules, *J. Phys. Chem. C* 114 (21) (2010) 9876–9882.
- [31] D.A. Gregory, Y. Zhang, P.J. Smith, X. Zhao, S.J. Ebbens, Reactive inkjet printing of biocompatible enzyme powered silk micro-rockets, *Small* 12 (30) (2016) 4048–4055.